

Utilizing encoding time as a resource to enhance quantum sensing by probe qubit dephasing

Ji-Bing Yuan,^{1,*} Hai-Fei Liu,¹ Ya-Ju Song,¹ Shi-Qing Tang,¹ Xin-Wen Wang,^{1,†} and Le-Man Kuang^{2,3,‡}

¹Key Laboratory of Opto-electronic Control and Detection Technology of University of Hunan Province, and College of Physics and Electronic Engineering, Hengyang Normal University, Hengyang 421002, China

²Key Laboratory of Low-Dimensional Quantum Structures and Quantum Control of Ministry of Education, and Department of Physics, Hunan Normal University, Changsha 410081, China

³Synergetic Innovation Academy for Quantum Science and Technology, Zhengzhou University of Light Industry, Zhengzhou 450002, China

(Dated: December 2, 2024)

We examine a system in which an impurity qubit is immersed in a quasi-two-dimensional dipolar Bose-Einstein condensate whose collective excitations act as a depasing reservoir for the qubit. The relative dipole-dipole interaction strength is estimated by the probe qubit dephasing. The ultimate precision of this estimation is quantified by the quantum Fisher information, which can be obtained by means of measuring quantum coherence of the probe qubit. Our findings indicate that, in the interval where roton excitations appear, the quantum Fisher information oscillates periodically with the encoding time t , and the amplitude of these oscillations increases alongside the extension of t . Moreover, we analytically determine that the envelope curve formed by the local maximum points satisfies the functional relationship $At + Bt^{1/2} + C$ during long-term encoding scenarios, where A, B, C are positive numbers. It is also revealed that the highly non-Markovian effects caused by the roton softening of the excitation spectrum allow long encoding time to serve as a resource for enhancing sensing precision. Our work provides a new pathway for enhancing the sensing precision of dephasing qubits.

I. INTRODUCTION

Quantum sensing aims to leverage quantum resources such as coherence [1, 2], entanglement [3–6], and squeezing [7, 8] to improve the precision of various physical measurements. It is essential to accurately sense various characteristic parameters of the environment surrounding a quantum system in quantum control and quantum information processing, as any quantum system inevitably interacts with its surrounding environment, leading to decoherence [9]. However, achieving this is challenging due to the numerous degrees of freedom in the environment. An effective strategy to address this challenge is the utilization of quantum probes, which are small, controllable, and measurable quantum systems [10–17]. A quantum probe is initially prepared in an appropriate state and then placed in the environment to interact. During this interaction, the information about the environment parameters to be estimated encodes into the quantum state of the probe. Finally, measurements are performed on the probe to extract this information. The precision of this estimation has been extensively studied using tools from quantum parameter estimation theory [18, 19]. According to the theory, the ultimate precision of any estimation procedure is constrained by the quantum Cramér-Rao (QCR) bound, which can be quantified by the quantum Fisher information (QFI) [20, 21]. A higher QFI indicates greater potential achievable precision.

As a simple and widely used quantum system, the qubits have attracted considerable attention as a quantum probe for sensing environments [22–31]. In many instances, when considering the interaction between the qubits and their environment without energy exchange, the dynamics of the probe can

be effectively described by a dephasing model. The dephasing qubits have been widely applied to detect various properties of reservoirs such as measuring ultra-low temperatures [32–35] and probing the cutoff frequency and coupling strength of Ohmic reservoirs [36–39]. In these sensing processes, the information about the parameter being measured is encoded into the decoherence factor of the qubits' evolving state. It is easy to infer that an initial short period of encoding time can enhance the precision of sensing. And if the coherence of the qubits degrades over extended encoding time, the sensing precision may decrease. In fact, in studies reported on the use of qubits dephasing for quantum sensing, there generally exist an optimal encoding time that maximizes the QFI. Therefore, these sensing schemes require precise control over the measurement time. In this work, we will demonstrate a novel dynamics of QFI when using a single qubit dephasing to sense the environment, suggesting that long encoding time can be used as a resource for enhancing sensing precision.

Owing to their unprecedented controllability and low temperature, atomic Bose-Einstein condensates (BECs) are often referred as the reservoirs suitable for engineering in both experimental [40–46] and theoretical [47–52] studies. In this work, we consider a system in which an impurity qubit is immersed in a quasi-two-dimensional (quasi-2D) dipolar BEC whose collective excitations act as a depasing reservoir for the qubit. We have shown that, by increasing the relative strength of the dipole-dipole interaction (DDI), the dephasing dynamics of the qubit changed from being Markovian to weak non-Markovian and eventually to highly non-Markovian. Especially, when roton excitations are present, the non-Markovianity becomes divergent [52]. Meanwhile, recent studies have demonstrated that non-Markovian effects have a positive impact on quantum sensing [53–57]. These findings inspire us to use the qubit dephasing for sensing the relative DDI. Our results show that, during the interval where roton excitations are present, the QFI oscillates periodically

* jbyuan@hynu.edu.cn

† xwwang@hynu.edu.cn

‡ lmkuang@hunnu.edu.cn

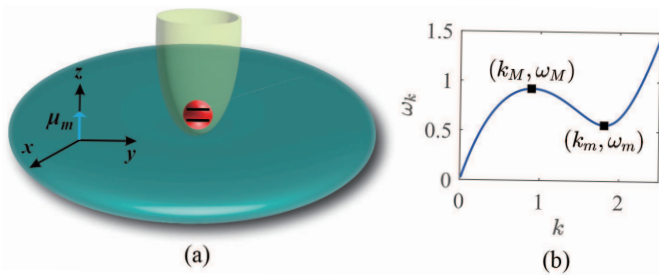


FIG. 1. (color online) Schematic diagrams of (a) an atomic qubit immersed in a quasi-2D dipolar BEC and (b) the typical roton spectrum of dipolar BECs with one minima (k_m, ω_m) and one maxima (k_M, ω_M) .

with encoding time t , and the amplitude of these oscillations increases as t extends. This indicates that extending the encoding time can enhance the precision of quantum sensing. Additionally, we derive an analytical expression for the QFI as a function of time and determine that the envelope curve formed by the local maximum points follows the functional relationship $At + Bt^{1/2} + C$ during long-term encoding scenarios, where A, B, C are positive numbers. We further point out that the highly non-Markovian effects caused by the roton softening of the excitation spectrum allow long encoding time to serve as a resource for enhancing sensing precision. This work offers a new approach for improving the sensing precision of dephasing qubits.

The paper is structured as follows: In Sec. II, we present the physical model of a single atomic qubit immersed in a thermally equilibrated quasi-2D dipolar atomic gas reservoir and propose the sensing scheme to estimate the relative DDI. Section III presents numerical and analytical results for the evolution of the QFI over time, demonstrating that encoding time can serve as a resource to enhance the precision of quantum sensing. Finally, a conclusion is given in Sec. IV.

II. QUANTUM SENSING PROTOCOL

As shown in Fig. 1(a), we consider a system in which a single atomic qubit is immersed in a thermally equilibrated quasi-2D dipolar atomic gas reservoir at temperature T . The qubit is confined in a harmonic trap $V_A(\mathbf{x}) = m_A \omega_A^2 \mathbf{x}^2 / 2$ that is independent of the internal states, where m_A is the mass of the impurity and ω_A is the trap frequency. For $\hbar \omega_A \gg k_B T$, the spatial wave function of the qubit is the ground state of $V_A(\mathbf{x})$, i.e., $\varphi_A(\mathbf{x}) = \pi^{-3/4} \ell_A^{-3/2} \exp[-\mathbf{x}^2 / (2\ell_A^2)]$ with $\ell_A = \sqrt{\hbar / (m_A \omega_A)}$. The Hamiltonian of the qubit is

$$\hat{H}_A = \hbar \Omega_A |e\rangle \langle e|,$$

where $\hbar \Omega_A$ is level splitting between the ground ($|g\rangle$) and excited ($|e\rangle$) states.

For the reservoir, we assume that each atom has a magnetic dipole moment μ_m polarized in the z direction. Conse-

quently, two atoms interact via the potential

$$V^{(3D)}(\mathbf{x} - \mathbf{x}') = g_B \delta(\mathbf{x} - \mathbf{x}') + \frac{3g_D}{4\pi} \frac{1 - 3\cos^2\theta}{|\mathbf{x} - \mathbf{x}'|^3},$$

where $g_B = 4\pi \hbar^2 a_B / m_B$ represents the contact interaction strength with m_B being the mass of the reservoir atom and a_B the s -wave scattering length, $g_D = \mu_0 \mu_m^2 / 3$ with μ_0 being the permeability of vacuum, and θ is the polar angle of $\mathbf{x} - \mathbf{x}'$. Additionally, the gas is confined along the z axis by the potential $V_B(z) = m_B \omega_z^2 z^2 / 2$, where ω_z is the trap frequency. For sufficiently large ω_z , the motion of the atoms along the z axis is frozen to the ground state of $V_B(z)$, i.e., $\varphi_B(z) = \pi^{-1/4} \ell_B^{-1/2} \exp[-z^2 / (2\ell_B^2)]$ with $\ell_B = \sqrt{\hbar / (m_B \omega_z)}$, effectively reducing the reservoir into a quasi-2D one. Finally, for small T , we assume that most of the reservoir atoms are condensed to zero momentum state with an area density n . Following Bogoliubov's method, the uncondensed atoms are then described by the quasiparticle Hamiltonian [58]

$$\hat{H}_B = \sum_{\mathbf{k} \neq 0} \hbar \omega_{\mathbf{k}} \hat{b}_{\mathbf{k}}^\dagger \hat{b}_{\mathbf{k}},$$

where $\mathbf{k} \equiv (k_x, k_y)$, $\hat{b}_{\mathbf{k}}$ is annihilation operator for the quasiparticle with wave vector \mathbf{k} , and excitation frequency is [59]

$$\omega_{\mathbf{k}} = \frac{1}{2} \sqrt{k^4 + P k^2 [1 + \chi \tilde{v}_D(k)]} \quad (1)$$

with $P = 8\sqrt{2}\pi \ell_B a_B n$ being a dimensionless parameter, $\tilde{v}_D(x) = 2 - 3\sqrt{\pi/2} x e^{x^2/2} \text{erfc}(x/\sqrt{2})$ being the Fourier transform of the effective 2D DDI, and

$$\chi = \frac{g_D}{g_B}$$

being the relative DDI strength. In this paper, we use ω_z as the unit of frequency and ℓ_B^{-1} as the unit of wave vector. It is now well-established that the sufficiently strong DDI would lead to the roton excitation and eventually the instability. In fact, for $P = 2$, roton excitation sets in when

$$\chi > \chi^* \simeq 4.23.$$

In addition, the condensate becomes unstable for $\chi > \chi^{**} = 5.67$. The typical roton spectrum is shown in Fig. 1(b).

For the qubit-reservoir coupling, we assume that the qubit undergoes s -wave collisions with reservoir atoms only when the qubit is in the excited state [47–50]. Let a_{AB} be the corresponding scattering length, the qubit-reservoir interaction Hamiltonian is then

$$\hat{H}_{AB} = \hbar \delta_e |e\rangle \langle e| + \hbar |e\rangle \langle e| \sum_{\mathbf{k} \neq 0} g_{\mathbf{k}} (\hat{b}_{\mathbf{k}} + \hat{b}_{\mathbf{k}}^\dagger),$$

where $\delta_e = 2\sqrt{\pi} n a_{AB} m_B \ell_B^2 / [m_{AB} (\ell_A^2 + \ell_B^2)^{1/2}]$ is the excited level shift due to the collision, $m_{AB} = m_A m_B / (m_A + m_B)$ is the reduced mass, and

$$g_{\mathbf{k}} = \frac{\delta_e}{\sqrt{2nS}} \frac{k e^{-\frac{\zeta^2 k^2}{4}}}{\sqrt{\omega_{\mathbf{k}}}} \quad (2)$$

is the qubit-reservoir coupling parameter, with S being the area of the reservoir and $\zeta = \ell_A/\ell_B$.

Now the total Hamiltonian, $\hat{H} = \hat{H}_A + \hat{H}_B + \hat{H}_{AB}$, is

$$\hat{H} = \hbar(\Omega_A + \delta_e)|e\rangle\langle e| + \sum_{\mathbf{k} \neq 0} \hbar\omega_{\mathbf{k}} \hat{b}_{\mathbf{k}}^\dagger \hat{b}_{\mathbf{k}} + \sum_{\mathbf{k} \neq 0} \hbar g_{\mathbf{k}} |e\rangle\langle e| (\hat{b}_{\mathbf{k}} + \hat{b}_{\mathbf{k}}^\dagger), \quad (3)$$

Since \hat{H}_A commutes with \hat{H}_{AB} , the dynamics of the impurity qubit in reservoir is purely dephasing. In the following we use the probe qubit dephasing to estimate the relative DDI strength χ and put forward the following quantum sensing protocol: (i) First we initialize the probe qubit in the superposition state $|\psi\rangle = (|g\rangle + |e\rangle)/\sqrt{2}$. (ii) Then the probe qubit undergoes a parameter-encoding process by interacting with the dipolar BEC. (iii) Finally, we perform a measurement $\hat{\sigma}_x$ on the probe qubit.

We now detail the sensing protocol. The initial state of the total system is prepared as

$$\hat{\rho}_{tot}(0) = |\psi\rangle\langle\psi| \otimes \hat{\rho}_B,$$

where $\hat{\rho}_B = \prod_{\mathbf{k}} (1 - e^{-\beta\omega_{\mathbf{k}}}) e^{-\beta\omega_{\mathbf{k}} \hat{b}_{\mathbf{k}}^\dagger \hat{b}_{\mathbf{k}}}$ is a thermal state of the BEC with $\beta = 1/k_B T$. For simplicity, we shall only consider the zero temperature case in this work. Let the whole system evolve under the control of the Hamiltonian (3) for a certain time $t/2$, after which a π -pulse about x is applied to the qubit. Then the system is allowed to evolve for the same time period $t/2$ and another π -pulse is applied. Through these processes, the quantum state of the probe qubit at time t can be given as

$$\hat{\rho}_A(t) = \frac{1}{2} \begin{pmatrix} 1 & e^{-\Gamma(t)} \\ e^{-\Gamma(t)} & 1 \end{pmatrix}, \quad (4)$$

where $\Gamma(t)$ is the decoherence factor with following expression

$$\Gamma(t) = \sum_{\mathbf{k} \neq 0} \frac{g_{\mathbf{k}}^2}{\omega_{\mathbf{k}}^2} [1 - \cos(\omega_{\mathbf{k}} t)]. \quad (5)$$

Here and henceforth, we adopt ω_z^{-1} as the unit of time.

From Eq. (1) and Eq. (5), we see that information of the relative DDI strength χ is encoded into the decoherence factor of the qubit. In the following, we introduce the quantum parameter estimate theory to quantify the sensing precision. As is well-known, the sensing precision of χ is restricted to the QCR bound

$$\delta\chi \geq \frac{1}{\sqrt{\nu \mathcal{F}_\chi^Q}}. \quad (6)$$

Here $\delta\chi$ is the mean square error, ν represents the number of repeated experiments and \mathcal{F}_χ^Q denotes QFI with respect to the χ . The QCR bound in Eq. (6) indicates that a larger amount of QFI corresponds to enhanced potential sensing precision. The QFI for state (4) is given as [20, 21]

$$\mathcal{F}_\chi^Q = \frac{(\partial_\chi \Gamma)^2}{e^{2\Gamma} - 1}. \quad (7)$$

In this paper, $\partial_x Y$ represents the partial derivative of Y with respect to x .

The final stage of the sensing protocol involves determining the optimal measurement $\hat{\Lambda}$ which can saturate the QCR bound. For a qubit system, the Fisher information associated with the measurement \hat{X} can be presented as [2]

$$\mathcal{F}_\chi = \frac{(\partial_\chi \langle \hat{X} \rangle)^2}{\langle \Delta \hat{X}^2 \rangle},$$

where $\langle \hat{X} \rangle$ and $\langle \Delta \hat{X}^2 \rangle$ are mean and variance of the measured observable, respectively. The QFI is the upper bound of the Fisher information associated with the measurement, i.e.,

$$\mathcal{F}_\chi^Q = \max_{\hat{X}} \mathcal{F}_\chi(\hat{X}) = \mathcal{F}_\chi(\hat{\Lambda}).$$

It can be proven that the Fisher information associated with the pauli matrices $\hat{\sigma}_x$ is exactly equal to the QFI given by Eq. (7) [32, 35]. Therefore, we shall choose $\langle \hat{\sigma}_x \rangle$ as the measurement signal, which can be observed using Ramsey interferometry [1, 43, 60].

III. QUANTUM SENSING ENHANCEMENT VIA LONG ENCODING TIME

A. Numerical results

In this subsection, we begin by examining the evolution of the decoherence factor over time. To achieve this, we perform a continuization process on the decoherence factor in Eq. (5). Substituting $g_{\mathbf{k}}$ in Eq. (2) into Eq. (5) and using the continuum limit $\frac{1}{S} \sum_{\mathbf{k}} \rightarrow \frac{1}{2\pi\ell_B^2} \int_0^\infty k dk$, the decoherence factor can be rewritten as

$$\Gamma(t) = Q \int_0^\infty f(k) \frac{[1 - \cos(\omega_k t)]}{\omega_k^3} dk \quad (8)$$

where $Q = na_{AB}^2 \ell_B^2 (m_A + m_B)^2 / [m_A^2 (\ell_A^2 + \ell_B^2)]$ is a dimensionless parameter measuring the qubit-reservoir coupling and $f(k) \equiv k^3 e^{-\zeta^2 k^2/2}$. Combining Eqs. (1) and (8), we know that the decoherence factor Γ is a function of t , χ , P , and Q . To fix P and Q , we consider a single ^{87}Rb atom immersed in a dipolar BEC ^{164}Dy atoms [61] which possess a magnetic dipole moment of $10\mu_B$. We assume a typical trap frequency $\omega_z = 2\pi \times 10^3$ Hz, the corresponding harmonic oscillator width is $\ell_B \simeq 2.5 \times 10^{-5}$ cm. Next, we consider a typical condensate peak density of 10^{14} cm $^{-3}$, the area density is then $n = 4.4 \times 10^9$ cm $^{-2}$. Consequently, we have $P \sim 1.5$. To find Q , we assume that the s -wave scattering length between ^{87}Rb and ^{164}Dy atoms is $a_{AB} \sim 5$ nm and the width of the impurity trap ℓ_A equals to ℓ_B ($\zeta = 1$), we therefore have $Q \sim 4.6 \times 10^{-3}$. Without loss of generality, we shall take $P = 2$ and $Q = 4 \times 10^{-3}$ in the results presented below. It has been verified that changing the values of P and Q would not change our main results qualitatively.

Based on Eq. (8), we plot the typical dynamical behaviors of $\Gamma(t)$ for various values of χ in Fig. 2. From the top four

subfigures, we can observe that as χ increases, the number of oscillations of Γ over time increases; but they all quickly converge to the asymptotic value after a few oscillations. The bottom four subfigures show us that when $\chi > \chi^*$ where the roton excitation appear, $\Gamma(t)$ becomes a damped oscillating function that oscillates for a very long period of time. The fact that $\Gamma(t)$ exhibits very distinct behaviors for different χ inspires us to use the qubit dephasing to estimate the relative DDI χ .

Figure 3 shows the dynamical behaviors of \mathcal{F}_χ^Q corresponding to the values of χ in Fig. 2. The top four subfigures demonstrate that there exist an optimal encoding time at which the QFI reaches its maximum, similar to the QFI dynamics studied previously [32–39]. However, when $\chi > \chi^*$, the bottom four subfigures show that the QFI oscillates periodically with the encoding time t , and the amplitude of these oscillations increases alongside the extension of t . In fact, we numerically find that this growth trend still holds for t over 1000. Moreover, by comparing the bottom four subfigures, we observe that the local maximum attainable value of QFI within the same time period increases as χ increases. Notably, when χ approaches χ^{**} , this maximum value rises sharply. These dynamical behaviors suggest that extending the encoding time can enhance quantum sensing precision within the range where roton excitations appear. And the degree of enhancement becomes more pronounced as χ is close to the unstable point χ^{**} .

B. Analytical findings

In this subsection, to gain a better understanding of why QFI increases with encoding time in the interval $\chi > \chi^*$, we attempt to derive an approximate analytical expression for the evolution of QFI over time. To achieve this, we divide $\Gamma(t)$ in Eq. (8) into two parts: the time-independent part

$$\Gamma_0 = Q \int_0^\infty \frac{f(k)}{\omega_k^3} dk$$

and the time-dependent part

$$\Gamma_1(t) = - \int_0^\infty G(\omega) \cos(\omega t) d\omega, \quad (9)$$

where $G(\omega)$ is given as

$$G(\omega) = Q \sum_i \frac{f(k_i(\omega))}{\omega^3} \left| \frac{d\omega_k}{dk} \right|_{k=k_i(\omega)}^{-1} \quad (10)$$

with $k_i(\omega)$ being the root of the equation $\omega_k = \omega$. As shown in Fig. 1(b), the roton spectrum has a minima (k_m, ω_m) and a maxima (k_M, ω_M). Based on Eq. (10), $G(\omega)$ diverges at ω_m and ω_M . To accurately take into account the contributions from these singularities to $G(\omega)$, let us focus on ω_k in the vicinities of k_m where the excitation energy can be approximated as $\omega_k \approx \hbar\omega_m + \omega_k''(k_m)(k - k_m)^2/2$. Using Eq. (10), it can be then shown that, in the vicinity of ω_m , we

have $G(\omega) \approx g_m(\omega_m - \omega)^{-1/2}$ for $\omega > \omega_m$, where

$$g_m = Q \sqrt{\frac{2}{|\omega_k''(k_m)|}} \frac{f(k_m)}{\omega_m^3}.$$

Similarly, in the vicinity of the maxima, we have $G(\omega) \approx g_M(\omega - \omega_M)^{-1/2}$ for $\omega < \omega_M$, where

$$g_M = Q \sqrt{\frac{2}{|\omega_k''(k_M)|}} \frac{f(k_M)}{\omega_M^3}.$$

Now, by assuming that these two singularities give rise to the largest contribution to $G(\omega)$, we define function

$$\tilde{G}(\omega) = g_m \frac{H(\omega - \omega_m)}{\sqrt{\omega - \omega_m}} + g_M \frac{H(\omega_M - \omega)}{\sqrt{\omega_M - \omega}} \quad (11)$$

as the approximate of $G(\omega)$, where $H(x)$ is the Heaviside step function. By substituting $\tilde{G}(\omega)$ for $G(\omega)$ in Eq. (9), we obtain an approximate $\Gamma_1(t)$

$$\tilde{\Gamma}_1(t) = - \sqrt{\frac{\pi}{t}} \left[g_m \cos\left(\omega_m t + \frac{\pi}{4}\right) + g_M \cos\left(\omega_M t - \frac{\pi}{4}\right) \right]. \quad (12)$$

The near-perfect overlap of curves $\Gamma_1(t)$ and $\tilde{\Gamma}_1(t)$ in Fig. 4 indicates that the approximation is valid. In fact, including other values of $\chi > \chi^*$, even if the time is extended to 1000, we find that such overlap would still be satisfied. The variations of ω_m, ω_M and g_m, g_M with χ are presented in Fig. 5 (a) and 5 (b), respectively. The decrease in ω_m with increasing χ observed in Fig. 5 (a) is termed as the roton mode softening [59].

Next, based on $\tilde{\Gamma}_1(t)$ in Eq. (12), we derive the analytical expression of QFI as a function of time for long-term encoding. Under long-term conditions ($t \gg 1$), neglecting the decay term related to time, we can obtain $e^{2\Gamma} \approx e^{2\Gamma_0}$ and

$$\partial_\chi \tilde{\Gamma}_1 \approx \sqrt{\pi t} \left[a_m \sin\left(\omega_m t + \frac{\pi}{4}\right) + a_M \sin\left(\omega_M t - \frac{\pi}{4}\right) \right],$$

where $a_i = g_i \partial_\chi \omega_i$ with $i = m, M$. From Fig. 6 (a), it is evident that $|a_m| \gg |a_M|$, allowing for the reasonable approximation as follows

$$\partial_\chi \tilde{\Gamma}_1 \approx \sqrt{\pi} a_m \sqrt{t} \sin\left(\omega_m t + \frac{\pi}{4}\right). \quad (13)$$

Due to $\partial_\chi \omega_m < 0$ and $g_m > 0$, a_m has to be negative. The change in $\lg(-a_m)$ as a function of χ is illustrated in Fig. 6 (b). Using Eq. (13), it is straightforward to derive an approximate expression for QFI in Eq. (7)

$$\tilde{\mathcal{F}}_\chi^Q = A t \sin^2\left(\omega_m t + \frac{\pi}{4}\right) - B \sqrt{t} \sin\left(\omega_m t + \frac{\pi}{4}\right) + C, \quad (14)$$

where A, B, C are time-independent parameters with following forms

$$A = \frac{\pi a_m^2}{e^{2\Gamma_0} - 1}, \quad B = \frac{2\sqrt{\pi} a_m \partial_\chi \Gamma_0}{1 - e^{2\Gamma_0}}, \quad C = \frac{(\partial_\chi \Gamma_0)^2}{e^{2\Gamma_0} - 1}.$$

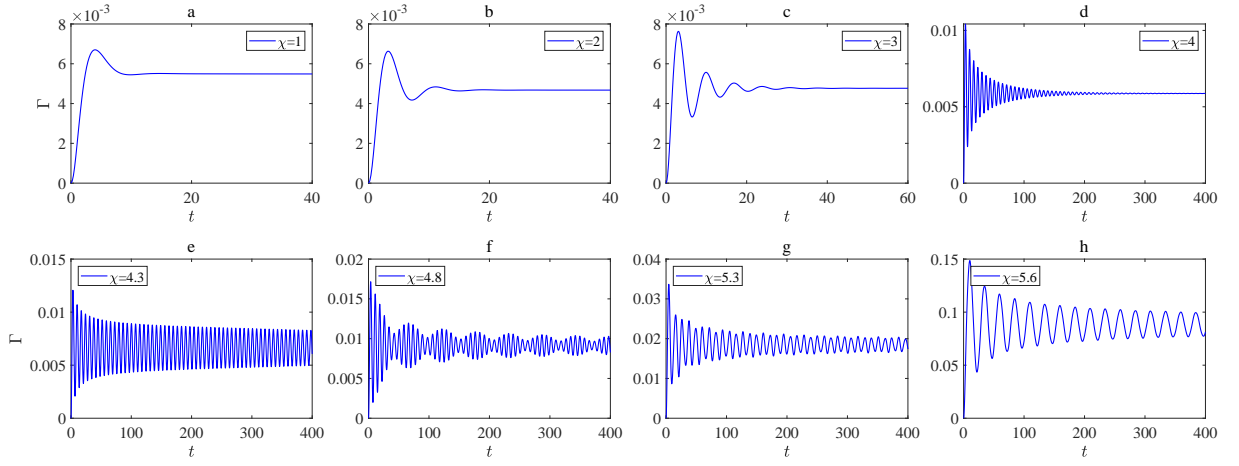


FIG. 2. (color online) Time dependence of the decoherence factor Γ for $\chi = 1$ (a), 2 (b), 3 (c), 4 (d), 4.3 (e), 4.8 (f), 5.3 (g), and 5.6 (h).

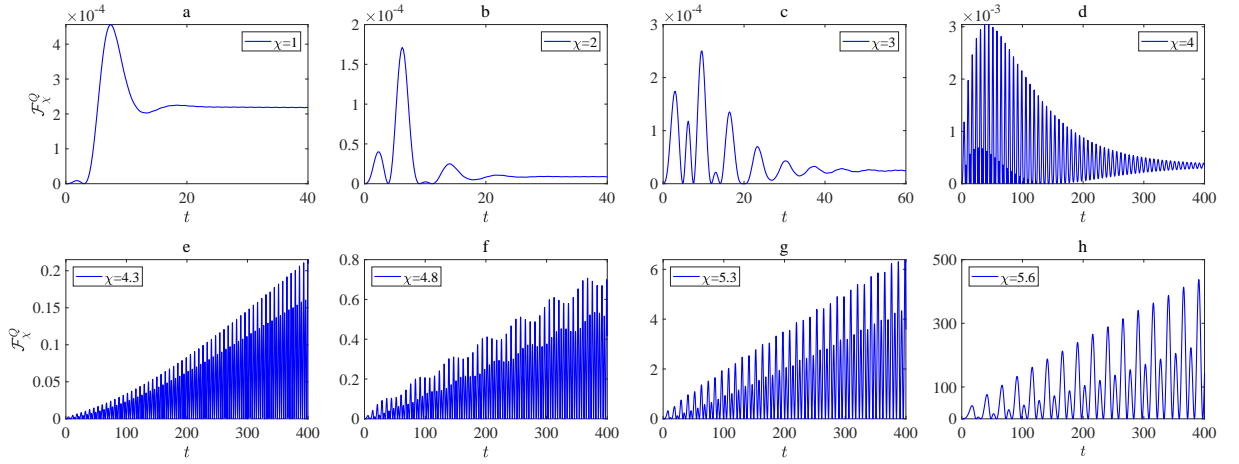


FIG. 3. (color online) Time dependence of the QFI \mathcal{F}_χ^Q for $\chi = 1$ (a), 2 (b), 3 (c), 4 (d), 4.3 (e), 4.8 (f), 5.3 (g), and 5.6 (h).

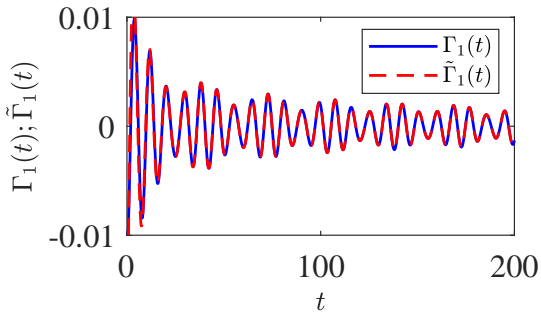


FIG. 4. (Color online). Comparison of $\Gamma_1(t)$ and $\tilde{\Gamma}_1(t)$ for $\chi = 4.8$. Parameters used are $\omega_m = 0.7971$, $\omega_M = 0.9114$, $g_m = 9.5 \times 10^{-3}$ and $g_M = 3.8 \times 10^{-3}$, where g_m and g_M are expressed in unit of $\omega_z^{-1/2}$.

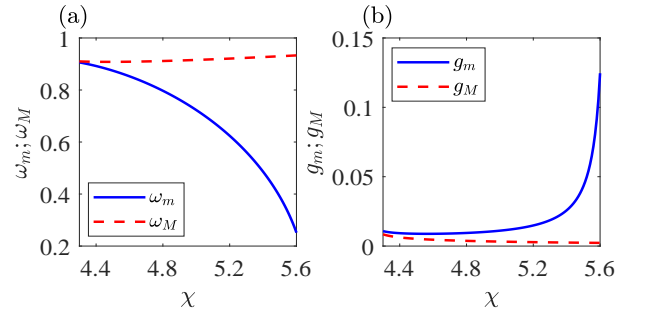


FIG. 5. (Color online). ω_m , ω_M in (a) and g_m , g_M (in unit of $\omega_z^{-1/2}$) in (b) versus χ .

time

$$t_{LO} = \frac{(2n + \frac{5}{4})\pi}{\omega_m}$$

The relationship between $\lg(A)$, $\lg(B)$, $\lg(C)$, and χ is depicted in Fig. 7. Clearly, A , B and C are all positive values. According to Eq. (14), it is easy to determine the local optimal

at which the QFI reaches a local maximum, where n is a positive integer. The corresponding local maximum of the QFI

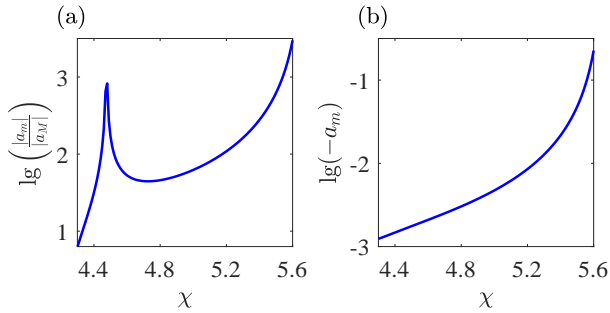


FIG. 6. (Color online). Plot of $\lg\left(\frac{a_m}{a_M}\right)$ in (a) and $\lg(-a_m)$ in (b) as a function of χ , where a_m and a_M are expressed in unit of $\omega_z^{1/2}$.

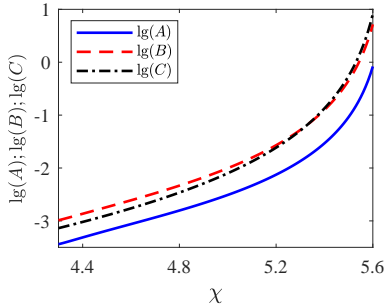


FIG. 7. (color online). Plot of $\lg(A)$, $\lg(B)$ and $\lg(C)$ as a function of χ . Here the unit for A is ω_z , and the unit for B is $\omega_z^{1/2}$.

reads

$$\tilde{\mathcal{F}}_\chi^Q(t_{LO}) = At_{LO} + B\sqrt{t_{LO}} + C. \quad (15)$$

Figure 7 illustrates that A , B , and C all increase by three orders of magnitude from $\chi = 4.3$ to $\chi = 5.6$, which exactly confirms the observation in Figs. 3 (e) to 3 (h) that the local maximum QFI in the same duration also increases by three orders of magnitude. Finally, to verify the validity of Eq. (14), we pick two point $\chi = 4.8$ in Fig. 8 (a) and $\chi = 5.6$ in Fig. 8 (b) to compare the dynamical behaviors of \mathcal{F}_χ^Q and $\tilde{\mathcal{F}}_\chi^Q$. The plot reveals that these two curves (blue solid line and red dashed line) are nearly identical, achieving an even greater congruence at $\chi = 5.6$. The black dash-dotted lines shown in Figs. 8 (a) and 8 (b) are governed by Eq. (15), which clearly indicates that the long encoding time can be a resource for enhancing quantum sensing precision.

C. Discussion

In this subsection, let's discuss the relationship between non-Markovian effects and the enhancement of quantum sensing via long encoding time. The non-Markovian effects refer to phenomena in which information flows from the environment back to the system, allowing the open quantum system to recover some of its lost memory [9]. Recent studies have shown that non-Markovian effects positively impact quantum sensing [53–57]. For a dephasing qubit, the non-Markovian

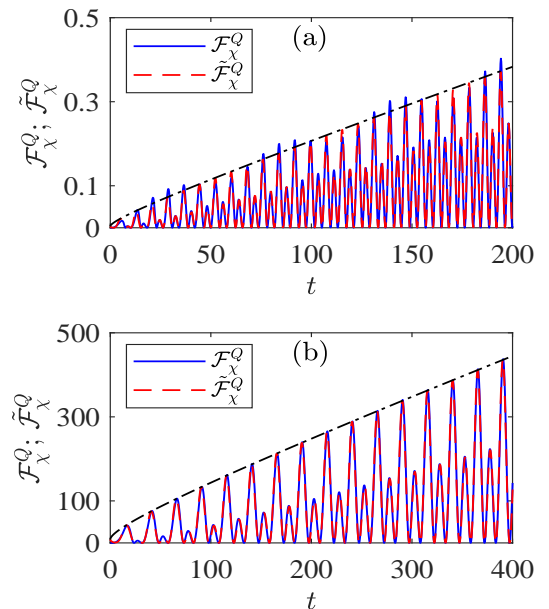


FIG. 8. (Color online). Comparison of \mathcal{F}_χ^Q and $\tilde{\mathcal{F}}_\chi^Q$ for $\chi = 4.8$ (a) and $\chi = 5.6$ (b). Parameters used in (a) are $\omega_m = 0.7971$, $A = 1.6 \times 10^{-3}$, $B = 4.6 \times 10^{-3}$, and $C = 3.4 \times 10^{-3}$ and in (b) are $\omega_m = 0.2515$, $A = 0.8316$, $B = 5.2028$, and $C = 8.1374$.

effects are manifested in the reduction of the decoherence factor over time. Based on reference [62], the measure of non-Markovianity is

$$\mathcal{N} = \int_{\Gamma'(t) < 0} de^{-\Gamma(s)},$$

where the integration is over all intervals in which $\Gamma'(t) < 0$. For a Markovian process, the decoherence factor either increases over time or increases to a constant value. These scenarios correspond to the QFI decreasing to zero with prolonged encoding time and remaining constant, respectively. Therefore, we can say that the presence of non-Markovian effects is a necessary condition for extending encoding time to enhance quantum sensing precision. In the interval $\chi < \chi^*$, the presence of non-Markovian effects for only a limited duration, as shown from Figs. 2 (a) to 2 (d), does not make long encoding time a resource for enhancing quantum sensing precision. This is confirmed by the dynamical behaviors of \mathcal{F}_χ^Q in Figs. 3 (a) to 3 (d). Fortunately, based on Eq. (12), it is found that in the interval $\chi > \chi^*$ where roton excitations appear, the non-Markovian effects exhibit the following two special properties: (i) The non-Markovian effects are present throughout the dephasing dynamics, implying that information is exchanged between the qubit probe and the dipolar BEC over a prolonged duration. (ii) The non-Markovianity \mathcal{N} is divergent. This can be proven using the inequality

$$\mathcal{N} > \epsilon \sum_{n=1}^{\infty} \frac{1}{\sqrt{n}},$$

where ϵ is a positive real number and infinite series $\sum_{n=1}^{\infty} 1/\sqrt{n}$ is divergent. We believe that such highly non-

Markovian effects enable long encoding time to serve as a resource for enhancing sensing precision .

IV. CONCLUSION

In this work, we considered a system where an impurity qubit is embedded in a quasi-2D dipolar BEC. The collective excitations of the dipolar BEC act as a dephasing reservoir for the qubit. By measuring the single-qubit dephasing, we estimated the relative strength of the DDI whose estimation precision is quantified by the QFI. We carefully examined the dynamical behaviors of the QFI at various values of χ . It has been shown that, in the region $\chi > \chi^*$ where roton excitations appear, the QFI oscillates and increases over time. This indicates that extending the encoding time can enhance the precision of quantum sensing. We derived a simple analytical expression for the time evolution of QFI in $\chi > \chi^*$, thereby determining that the envelope curve formed by the local maximum points satisfies the functional relationship $At + Bt^{1/2} + C$ during long-term encoding scenarios. It was found that A , B , and C are all positive numbers and all increased by three orders of magnitude as χ varied from 4.3 to 5.6. Particularly, as χ approaches χ^{**} , the rate of increase becomes significantly steeper. It was found that the non-Markovian effects caused by the roton softening of the excitation spectrum have two special properties: (i) The non-

Markovian effects are present throughout the dephasing dynamics. (ii) The non-Markovianity \mathcal{N} is divergent. We believe that such highly non-Markovian effects enable long encoding time to serve as a resource for enhancing sensing precision.

Finally, we note that roton-like dispersions are also found in atomic condensates placed inside an optical cavity [63] or with spin-orbit coupling [64]. Therefore, when utilizing dephasing qubits to estimate certain parameters of these systems, long encoding time may also serve as a resource for enhancing quantum sensing precision. Our work provides a new pathway for enhancing the sensing precision of dephasing qubits.

ACKNOWLEDGMENTS

J. B. Yuan was supported by NSFC (No. 11905053) and Scientific Research Fund of Hunan Provincial Education Department of China under Grant (No. 21B0647). L. M. Kuang was supported by NSFC (Nos. 12247105, 1217050862, and 11935006) and the science and technology innovation Program of Hunan Province (No. 2020RC4047). Y. J. Song was supported by NSFC (No. 12205088) and Scientific Research Fund of Hunan Provincial Education Department of China under Grant (No. 21B0639). S. Q. Tang was supported by Scientific Research Fund of Hunan Provincial Education Department of China under Grant (No. 22A0507).

-
- [1] D. Adam, Q. Bouton, J. Nettersheim, S. Burgardt, and A. Widera, Coherent and dephasing spectroscopy for single impurity probing of an ultracold bath, *Phys. Rev. Lett.* 129, 120404 (2022).
 - [2] M. T. Mitchison, T. Fogarty, G. Guarnieri, S. Campbell, T. Busch, and J. Goold, In situ thermometry of a cold Fermi gas via dephasing impurities, *Phys. Rev. Lett.* 125, 080402 (2020).
 - [3] T. Nagata, R. Okamoto, J. L. O'Brien, K. Sasaki, and S. Takeuchi, Beating the standard quantum limit with four-entangled photons, *Science* 316, 726 (2007).
 - [4] L. Pezzè, A. Smerzi, M. K. Oberthaler, R. Schmied, and P. Treutlein, Quantum metrology with nonclassical states of atomic ensembles, *Rev. Mod. Phys.* 90, 035005 (2018).
 - [5] S. A. Haine and J. J. Hope, Machine-designed sensor to make optimal use of entanglement-generating dynamics for quantum sensing, *Phys. Rev. Lett.* 124, 060402 (2020).
 - [6] G. Planella, M. F. B. Cenni, A. Acin, and M. Mehboudi, Bath-induced correlations enhance thermometry precision at low temperatures, *Phys. Rev. Lett.* 128, 040502 (2022).
 - [7] W. Muessel, H. Strobel, D. Linnemann, D. B. Hume, and M. K. Oberthaler, Scalable spin squeezing for quantum-enhanced magnetometry with Bose-Einstein Condensates, *Phys. Rev. Lett.* 113, 103004 (2014).
 - [8] K. Bai, Z. Peng, H. G. Luo, and J. H. An, Retrieving ideal precision in noisy quantum optical metrology, *Phys. Rev. Lett.* 123, 040402 (2019).
 - [9] H. P. Breuer and F. Petruccione, *The Theory of Open Quantum Systems* (Oxford University Press, Oxford, 2007).
 - [10] C. Benedetti, F. Buscemi, P. Bordone, and M. G. A. Paris, Quantum probes for the spectral properties of a classical environment, *Phys. Rev. A* 89, 032114 (2014).
 - [11] M. Bina, F. Grasselli, and M. G. A. Paris, Continuous-variable quantum probes for structured environments, *Phys. Rev. A* 97, 012125 (2018).
 - [12] M. Mehboudi, A. Lampo, C. Charalambous, L. A. Correa, M. Á. García-March, and M. Lewenstein, Using polarons for sub-nK quantum nondemolition thermometry in a Bose-Einstein Condensate, *Phys. Rev. Lett.* 122, 030403 (2019).
 - [13] M. M. Khan, M. Mehboudi, H. Terças, M. Lewenstein, and M. A. Garcia-March, Subnanokelvin thermometry of an interacting d -dimensional homogeneous Bose gas, *Phys. Rev. Research* 4, 023191 (2022).
 - [14] Q. S. Tan, J. B. Yuan, J. Q. Liao, and L. M. Kuang, Super-sensitive estimation of the coupling rate in cavity optomechanics with an impurity-doped Bose-Einstein condensate, *Opt. Express* 28, 22867 (2020).
 - [15] Q. S. Tan, W. Wu, L. Xu, J. Liu, and L. M. Kuang, Quantum sensing of supersensitivity for the Ohmic quantum reservoir, *Phys. Rev. A* 106, 032602 (2022).
 - [16] J. B. Yuan, Z. M. Tang, Y. J. Song, S. Q. Tang, Z. H. Peng, X. W. Wang and L. M. Kuang, Antisymmetry-breaking-coupling-enhanced sensing of quantum reservoirs, *Phys. Rev. A* 110, 012613 (2024).
 - [17] N. Zhang, S. Y. Bai, and Chong Chen, Temperature-heat uncertainty relation in nonequilibrium quantum thermometry, *Phys. Rev. A* 110, 012211 (2024).
 - [18] C. W. Helstrom, *Quantum Detection and Estimation Theory* (Academic, New York, 1976).
 - [19] A. S. Holevo, *Probabilistic and Statistical Aspects of Quantum Theory* (North-Holland, Amsterdam, 1982).

- [20] W. Zhong, Z. Sun, J. Ma, X. G. Wang, and F. Nori, Fisher information under decoherence in Bloch representation, *Phys. Rev. A* 87, 022337 (2013).
- [21] J. Liu, H. D. Yuan, X. M. Lu, and X. G. Wang, Quantum Fisher information matrix and multiparameter estimation, *Journal of Physics A: Mathematical and Theoretical* 53, 023001 (2019).
- [22] S. Jevtic, D. Newman, T. Rudolph, and T. M. Stace, Single-qubit thermometry, *Phys. Rev. A* 91, 012331 (2015).
- [23] S. Fernandez-Lorenzo and D. Porras, Quantum sensing close to a dissipative phase transition: Symmetry breaking and criticality as metrological resources, *Phys. Rev. A* 96, 013817 (2017).
- [24] D. Tamascelli, C. Benedetti, H. P. Breuer, and M. G. A. Paris, Quantum probing beyond pure dephasing, *New Journal of Physics* 22, 083027 (2020).
- [25] Y. Chu, Y. Liu, H. Liu, and J. Cai, Quantum sensing with a single-qubit pseudo-Hermitian system, *Phys. Rev. Lett.* 124, 020501 (2020).
- [26] S. P. Wolski, D. Lachance-Quirion, Y. Tabuchi, S. Kono, A. Noguchi, K. Usami, and Y. Nakamura, Dissipation-based quantum sensing of magnons with a superconducting qubit, *Phys. Rev. Lett.* 125, 117701 (2020).
- [27] W. Wu and C. Shi, Quantum parameter estimation in a dissipative environment, *Phys. Rev. A* 102, 032607 (2020).
- [28] F. Chapeau-Blondeau, Quantum parameter estimation on coherently superposed noisy channels, *Phys. Rev. A* 104, 032214 (2021).
- [29] W. T. He, H. Y. Guang, Z. Y. Li, R. Q. Deng, N. N. Zhang, J. X. Zhao, F. G. Deng, and Q. Ai, Quantum metrology with one auxiliary particle in a correlated bath and its quantum simulation, *Phys. Rev. A* 104, 062429 (2021).
- [30] J. H. Lu, W. Ning, X. Zhu, F. Wu, L. T. Shen, Z. B. Yang, and S. B. Zheng, Critical quantum sensing based on the Jaynes-Cummings model with a squeezing drive, *Phys. Rev. A* 106, 062616 (2022).
- [31] Y. Aiache, A. E. Allati, and K. E. Anouz, Harnessing coherence generation for precision single- and two-qubit quantum thermometry, *Phys. Rev. A* 110, 032605 (2024).
- [32] S. Razavian, C. Benedetti, M. Bina, Y. Akbari-Kourbolagh, and M. G. A. Paris, Quantum thermometry by single-qubit dephasing, *Eur. Phys. J. Plus* 134, 284 (2019).
- [33] F. Gebbia, C. Benedetti, F. Benatti, R. Floreanini, M. Bina, and M. G. A. Paris, Two-qubit quantum probes for the temperature of an ohmic environment, *Phys. Rev. A* 101, 032112(2020).
- [34] A. Candeloro and M. G. A. Paris, Discrimination of Ohmic thermal baths by quantum dephasing probes, *Phys. Rev. A* 103, 012217 (2021).
- [35] J. B. Yuan, B. Zhang, Y. J. Song, S. Q. Tang, X. W. Wang and L. M. Kuang, Quantum sensing of temperature close to absolute zero in a Bose-Einstein condensate, *Phys. Rev. A* 107, 063317 (2023).
- [36] C. Benedetti, F. Salari Sehdaran, M. H. Zandi, and M. G. A. Paris, Quantum probes for the cutoff frequency of Ohmic environments, *Phys. Rev. A* 97, 012126 (2018).
- [37] F. S. Sehdaran, M. Bina, C. Benedetti, and M. G. A. Paris, Quantum probes for Ohmic environments at thermal equilibrium, *Entropy* 21, 486 (2019).
- [38] F. S. Sehdaran, M. H. Zandi, and A. Bahrapour, The effect of probe-Ohmic environment coupling type and probe information of the cutoff frequency, *Phys. Lett. A* 383, 126006 (2019).
- [39] H. Ather and A. Z. Chaudhry, Improving the estimation of environment parameters via initial probe-environment correlations, *Phys. Rev. A* 104, 012211 (2021).
- [40] S. Palzer, C. Zipkes, C. Sias, and M. Köhl, Quantum transport through a Tonks-Girardeau gas, *Phys. Rev. Lett.* 103, 150601 (2009).
- [41] S. Will, T. Best, S. Braun, U. Schneider, and I. Bloch, Coherent interaction of a single Fermion with a small bosonic field, *Phys. Rev. Lett.* 106, 115305 (2011).
- [42] N. Spethmann, F. Kindermann, S. John, C. Weber, D. Meschede, and A. Widera, Dynamics of single neutral impurity atoms immersed in an ultracold gas, *Phys. Rev. Lett.* 109, 235301 (2012).
- [43] R. Scelle, T. Rentrop, A. Trautmann, T. Schuster, and M. K. Oberthaler, Motional coherence of fermions immersed in a Bose gas, *Phys. Rev. Lett.* 111, 070401 (2013).
- [44] C. Zipkes, S. Palzer, C. Sias, and M. Köhl, A trapped single ion inside a Bose-Einstein condensate, *Nature (London)* 464, 388 (2010).
- [45] S. Schmid, A. Härter, and J. H. Denschlag, Dynamics of a cold trapped ion in a Bose-Einstein Condensate, *Phys. Rev. Lett.* 105, 133202 (2010).
- [46] J. B. Balewski, A. T. Krupp, A. Gaj, D. Peter, H. P. Büchler, Robert Löw, S. Hofferberth, and T. Pfau, Coupling a single electron to a Bose-Einstein condensate, *Nature (London)* 502, 664 (2013).
- [47] A. Recati, P. O. Fedichev, W. Zwerger, J. von Delft, and P. Zoller, Atomic quantum dots coupled to a reservoir of a superfluid Bose-Einstein Condensate, *Phys. Rev. Lett.* 94, 040404 (2005).
- [48] M. A. Cirone, G. De Chiara, G. M. Palma, and A. Recati, Collective decoherence of cold atoms coupled to a Bose-Einstein condensate, *New J. Phys.* 11, 103055 (2009).
- [49] P. Haikka, S. McEndoo, G. De Chiara, G. M. Palma, and S. Maniscalco, Quantifying, characterizing, and controlling information flow in ultracold atomic gases, *Phys. Rev. A* 84, 031602(R) (2011).
- [50] P. Haikka, S. McEndoo, and S. Maniscalco, Non-Markovian probes in ultracold gases, *Phys. Rev. A* 87, 012127 (2013).
- [51] Y. J. Song and L. M. Kuang, Controlling decoherence speed limit of a single impurity atom in a Bose-Einstein-Condensate Reservoir, *Ann. Phys.* 531, 1800423 (2019).
- [52] J. B. Yuan, H. J. Xing, L. M. Kuang, and S. Yi, Quantum non-Markovian reservoirs of atomic condensates engineered via dipolar interactions, *Phys. Rev. A* 95, 033610 (2017).
- [53] Z. Z. Zhang and W. Wu, Non-Markovian temperature sensing, *Phys. Rev. Research* 3, 043039 (2021).
- [54] W. Wu, S. Y. Bai, and J. H. An, Non-Markovian sensing of a quantum reservoir, *Phys. Rev. A* 103, L010601 (2021).
- [55] N. Zhang, C. Chen, S. Y. Bai, W. Wu, and J. H. An, Non-Markovian quantum thermometry, *Phys. Rev. Applied* 17, 034073 (2022).
- [56] L. Xu, J. B. Yuan, S. Q. Tang, W. Wu, Q. S. Tan, and L. M. Kuang, Non-Markovian enhanced temperature sensing in a dipolar Bose-Einstein condensate, *Phys. Rev. A* 108, 022608 (2023).
- [57] Y. Aiache, C. Seida, K. El Anouz, and A. E. Allati, Non-Markovian enhancement of nonequilibrium quantum thermometry, *Phys. Rev. E* 110, 024132 (2024).
- [58] D. van Oosten, P. van der Straten, and H. T. C. Stoof, Quantum phases in an optical lattice, *Phys. Rev. A* 63, 053601 (2001).
- [59] U. R. Fischer, Stability of quasi-two-dimensional Bose-Einstein condensates with dominant dipole-dipole interactions, *Phys. Rev. A* 73, 031602(R) (2006).
- [60] M. Cetina, M. Jag, R. S. Lous, I. Fritsche, J. T.M. Walraven, R. Grimm, J. Levinsen, M. M. Parish, R. Schmidt, M. Knap, and E. Demler, Ultrafast many-body interferometry of impurities coupled to a Fermi sea, *Science* 354, 96 (2016).
- [61] M. Lu, N. Q. Burdick, S. Ho Youn, and B. L. Lev, Strongly dipolar Bose-Einstein condensate of Dysprosium, *Phys. Rev.*

- Lett. 107, 190401 (2011).
- [62] H. P. Breuer, E. M. Laine, and J. Piilo, Measure for the degree of non-Markovian behavior of quantum processes in open systems, *Phys. Rev. Lett.* 103, 210401 (2009).
- [63] R. Mottl, F. Brennecke, K. Baumann, R. Landig, T. Donner, and T. Esslinger, Roton-type mode softening in a quantum gas with cavity-mediated long-range interactions, *Science* 336, 1570 (2012).
- [64] S. C. Ji, L. Zhang, X. T. Xu, Z. Wu, Y. J. Deng, S. Chen, and J. W. Pan, Softening of roton and phonon modes in a Bose-Einstein condensate with spin-orbit coupling, *Phys. Rev. Lett.* 114, 105301 (2015).